Indian Journal of Chemistry
Vol. 54A, April 2015, pp. 469-477

Crystallization of amorphous silica to silicalite-1: Effect of nature of silica sources and tetrapropylammonium hydroxide concentration

M S M Kamil[a], K Manikandan[a], S P Elangovan[b], Masaru Ogura[c], K K Cheralathan[a,*]

[a]Materials Chemistry Division, School of Advanced Sciences, VIT University, Vellore, 632 014, India
Email: cheralathan.k@vit.ac.in

[b]Department of Chemical System Engineering, The University of Tokyo, 7-3-1 Hongo, Bunkyo-ku, Tokyo, Japan
[c]Institute of Industrial Science, The University of Tokyo, Komaba 4-6-1, Meguro, Tokyo 153-8505, Japan

Received 29 April 2014; revised and accepted 23 March 2015

Dry gels obtained from different sources of silica such as SBA-15, SBA-16, fumed silica and tetraethyl orthosilicate have been crystallized into silicalite-1 by steam assisted conversion and characterized by powder X-ray diffraction, Fourier transform infrared spectroscopy , nitrogen adsorption, and high resolution scanning electron microscopy. The results show that the nature of source and concentration of tetrapropylammonium hydroxide have a significant effect on shape, size and pore structure of silicalite-1. ^{29}Si MAS NMR spectra of the dry gels obtained from different sources show that Si environment in these gels is similar. However, the morphology of silicalite-1 prepared under same experimental conditions is found to differ for different sources. Further, it is observed that silicalite-1 particles obtained from same source but under different TPAOH concentrations, exhibit different shapes and sizes. N_2 adsorption results reveal that the prepared silicalite-1 samples possess a wide pore size distribution and comprise pores in meso- and macro-pore regions, apart from zeolitic micropores.

Keywords: Zeolites, Mesoporous materials, Macroporous materials, Silicalite-1, Silica

In the recent years, zeolites having meso- and macro-pores have become highly desirable owing to their superior mass transfer properties and lower restrictions for the diffusion of reactants in adsorption/separation and catalytic applications[1-6]. The mesopores and the macropores may be present on zeolite crystals (intracrystalline) or in between the aggregated zeolite crystals (intercrystalline)[7]. Zeolites with meso- and macro- pores can be prepared by different approaches as reviewed by several researchers[6-9]. The preparation methodologies can be broadly classified into templated and non-templated. Soft templating[10-12], hard templating with carbonaceous templates[13-15], polymeric templating[16-18] and templating with other solids[19-21] are some examples of strategies employed by using templates. In the case of non-templated approaches, desilication[22-23], zeolitization of preformed solids[24-27] and silanization[28-30] methods have been reported.

Conversion of the preformed aluminosilicate dry gels into zeolites can be done by steam assisted conversion (SAC). In SAC, the dry gel containing aluminosilicate and organic structure directing agent (SDA) is crystallized in the presence of steam[31]. SAC method has been used for the preparation of pure silica zeolite such as silicalite-1 as well[32]. In SAC method since the gel is dried, mobility of the reaction species is highly reduced and their local concentration maximized. The high concentration of the reaction species is the ideal condition for massive nucleation[33]. Based on this strategy, aggregates of nanocrystalline zeolite beta that form mesoporous network have been prepared from aluminosilicate dry gel without the need of additional porogen[33]. However there is not much work found in the literature on the mechanistic aspects related to SAC. Further, to the best of our knowledge, effect of structure of silica sources on textural properties of zeolites has not been reported in the literature. Keeping this in mind, in the present work, dry gels obtained by mixing tetrapropyl-ammonium hydroxide (TPAOH) with SBA-15, SBA-16, fumed silica and tetraethyl orthosilicate (TEOS) were converted into silicalite-1 by steam assisted conversion. The influence of nature of silica sources and the effect of TPAOH concentration on the conversion of the amorphous silica sources to crystalline silicalite-1 was studied. The study indicated that apart from TPAOH concentration, the nature of silica sources also influences the morphology and pore structure of the prepared

zeolite. Further it was found that silicalite-1 with multimodal porosity can be obtained without use of any mesopore or macropore inducing templates.

Materials and Methods

Preparation of silicalite-1

SBA-15 and SBA-16 were synthesized using tetraethyl orthosilicate (TEOS) (≥ 99.9%, Sigma-Aldrich) as silica source and amphiphilic triblock copolymers, Pluronic P123 (Sigma-Aldrich) and F127 (Sigma-Aldrich) as structure directing agents according to the synthesis procedure reported elsewhere[34]. The silica source (weight of SiO_2 was 0.5 g) was mixed with appropriate quantity of tetrapropylammonium hydroxide (TPAOH) (1 *M* solution in water, Sigma-Aldrich) to get the gel. The gel was then dried at 373 K overnight to get the dry gel. TEOS, fumed silica (powder, particle size 0.014 μm, Sigma-Aldrich), calcined SBA-15, and calcined SBA-16 were used as silica sources. The TPAOH/Si molar ratio was varied as 0.5, 0.25, 0.125, 0.063, and 0.031. In a typical SAC procedure, the dried gel taken in a vial was placed inside a Teflon lined autoclave containing 2 mL distilled water. The vial was kept in such a manner that there was no direct contact between the dry gel and water. The autoclave was closed and placed in a hot air oven at 443 K for about 36 h. After the pre-fixed crystallization period, the autoclave was taken out and quenched to room temperature. Then the product was collected, and calcined at 823 K for 5 h in air to remove TPAOH.

Characterisation

Low and wide angle X-ray diffraction (XRD) patterns of the samples were obtained using Bruker, D8 advance X-ray diffractometer. Nitrogen adsorption measurements were carried out using a Quantachrome Autosorb-1 instrument at 77 K. Prior to adsorption, the samples were out gassed at 300 °C for 4 h. High resolution scanning electron microscope (HRSEM) images were captured using a FE I Quanta FEG 200 high resolution scanning electron microscope. ^{29}Si MAS NMR spectra of the dry gels containing TPAOH were collected on a Bruker DSX-300, NMR spectrometer. FTIR spectra were recorded using Shimadzu IR affinity-1 instrument. The samples were diluted with KBr and made into pellets before recording the IR spectra.

Results and Discussion

Characterization of the mesoporous silicas

The low angle XRD patterns and N_2 adsorption isotherms of mesoporous silicas, SBA-15 and SBA-16 are depicted in Fig. 1. The low angle XRD patterns and shape of the N_2 isotherms are typical of the mesoporous silicas and confirm the 2D-hexagonal and 3D-cubic mesostructure of SBA-15 and SBA-16 respectively[34]. The BET surface areas obtained from N_2 adsorption isotherms of SBA-15 and SBA-16 are 600 and 617 m^2/g respectively. The HRSEM images of the mesoporous silicas are presented in Fig. 2. SBA-15 consists of rod shaped particles with an average length

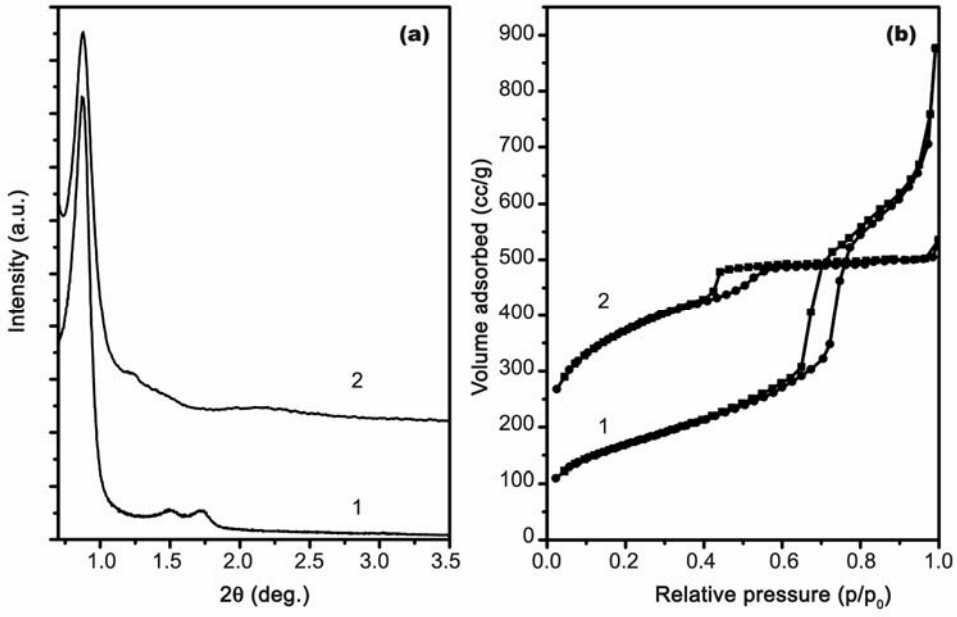

Fig. 1 – (a) Low angle XRD and (b) N_2 adsorption isotherms of mesoporous silicas. [(1) SBA-15; (2) SBA-16].

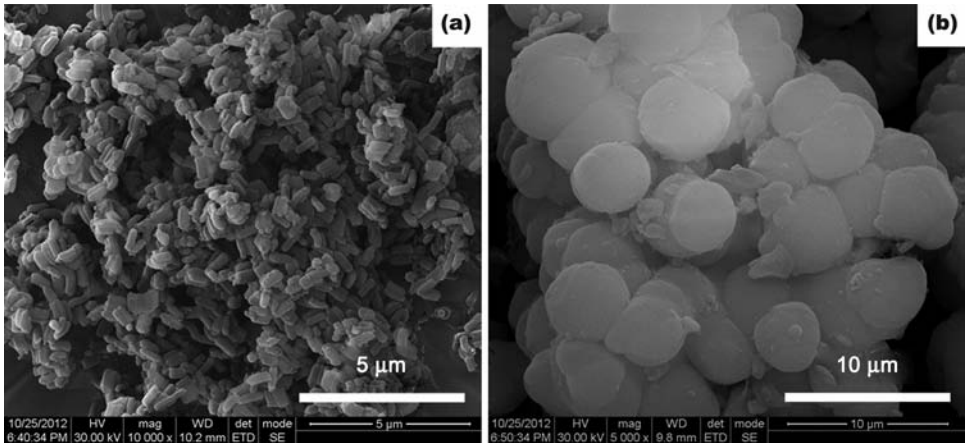

Fig. 2 – HRSEM images of mesoporous silicas. [(a) SBA-15; (b) SBA-16].

of 700 nm, while the particles of SBA-16 are spherical in shape with diameters ranging from 3 to 6 µm.

XRD patterns of silicalite-1

X-ray diffraction patterns of silicalite-1 samples obtained from SBA-15 with different TPAOH concentrations are shown in Fig. 3. Except for the sample obtained with TPAOH/Si molar ratio of 0.031, all the others show diffraction peaks corresponding to MFI topology[35]. The absence of diffraction peaks in the sample prepared with TPAOH/Si molar ratio of 0.031 indicates the absence of zeolite formation after SAC. In the case of silicalite-1 prepared with TPAOH/Si molar ratio of 0.063, the diffraction peaks overlap with amorphous silica background indicating partial crystallization. Since TPAOH is acting as a structure directing agent for the formation of silicalite-1, its concentration is critical and this may be the reason why crystallization is hampered at low TPAOH concentrations. XRD patterns of silicalite-1 samples prepared from different silica sources with the same TPAOH/Si molar ratio of 0.25 are presented in Fig. 4. The shape and position of the diffraction peaks confirm MFI topology of the prepared zeolites[35].

FTIR spectra of silicalite-1

FTIR spectra (lattice vibration region) of the silicalite-1 samples prepared from different silica sources with TPAOH/Si molar ratio of 0.25 are shown in the Fig. 5. In the spectra, the peaks at 1225 and 1107 cm^{-1} may be assigned to external and internal asymmetric stretching of T-O-T[36]. The peak appearing at 800 cm^{-1} may be correlated to symmetric stretching of T-O-T[36]. The bands in 450-460 cm^{-1} region may be assigned to T-O bending vibration[36]. In fully crystalline micrometer sized MFI zeolites, the

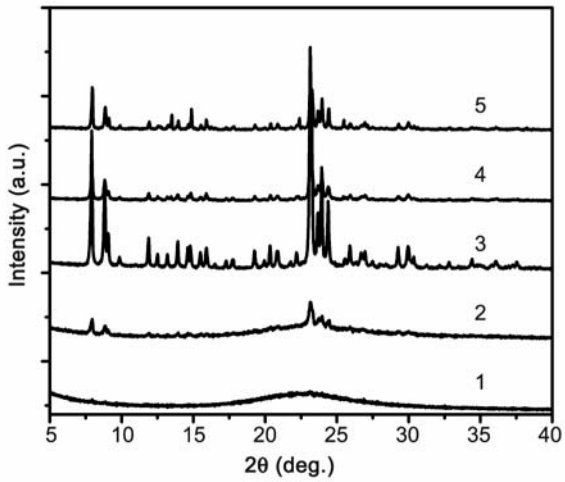

Fig. 3 – XRD patterns of the crystallized dry gels obtained from SBA-15 with different TPAOH/Si molar ratios. [(1) 0.031; (2) 0.063; (3) 0.125; (4) 0.25; (5) 0.5].

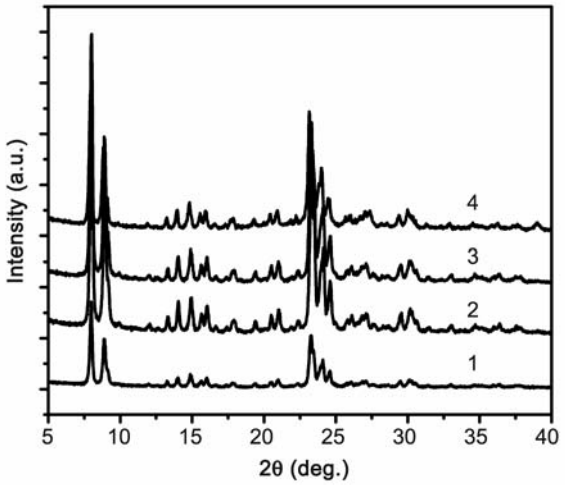

Fig. 4 – XRD patterns of calcined silicalite-1 samples obtained from different silica sources. [TPAOH/Si molar ratio = 0.25. (1) TEOS; (2) fumed silica; (3) SBA-15; (4) SBA-16].

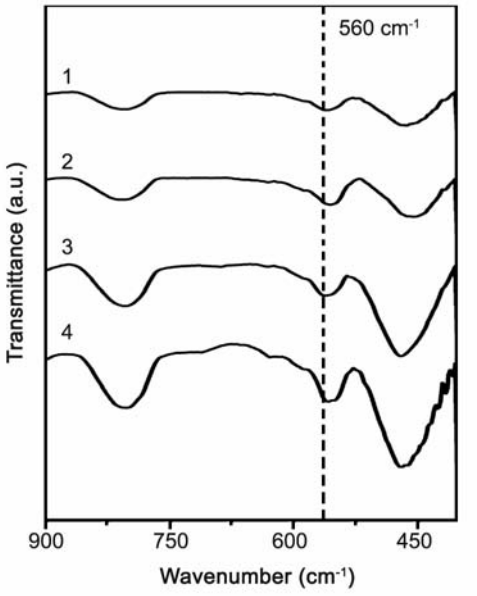

Fig. 5 – FTIR spectra of silicalite-1 samples obtained from different silica sources. [TPAOH/Si molar ratio = 0.25. (1) TEOS; (2) fumed silica; (3) SBA-15; (4) SBA-16].

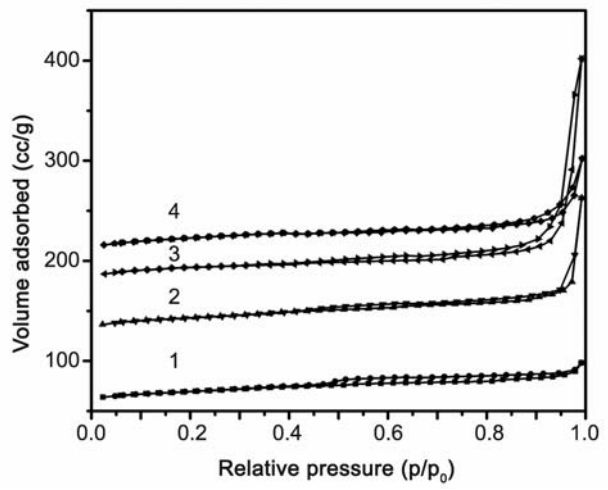

Fig. 6 – N_2 adsorption isotherms of silicalite-1 samples obtained from SBA-15 with different TPAOH/Si molar ratios. [(1) 0.063; (2) 0.125; (3) 0.25; (4) 0.5].

Table 1–N_2 adsorption data of silicalite-1 samples prepared from SBA-15 under different TPAOH/Si molar ratios

No.	TPAOH/Si molar ratio	BET surface area (m^2/g)	Mesopore area (m^2/g)	Micropore area (m^2/g)	Micropore vol. (cc/g)	Total pore vol. (cc/g)
1	0.5	224	71	153	0.08	0.23
2	0.25	274	47	226	0.123	0.46
3	0.125	282	63	219	0.116	0.32
4	0.063	212	58	154	0.082	0.154

pentasil (double five membered rings (D5R)) vibration band normally appears at 550 $cm^{-1}$and is used to confirm the formation of MFI structure[36]. It has been shown that when nanosized MFI particles are present, the pentasil band shifts to higher wavenumbers and also, the band may split into two peaks[37,38]. In the present study, the pentasil band appears at 560 cm^{-1} and the splitting (560 cm^{-1} and 548 cm^{-1}) is visible in samples obtained from SBA-16. The above observations confirm MFI topology of the prepared zeolites and further indicate nanosize of the particles.

N_2 adsorption of the silicalite-1

Nitrogen adsorption isotherms of silicalite-1 samples obtained from SBA-15 with different TPAOH concentrations are shown in Fig. 6. All the samples prepared from SBA-15 exhibit type I isotherm. In Fig. 6, disappearance of the hysteresis, originally observed in SBA-15 (see Fig.1(b)) can be observed, indicating disappearance of the mesostructure of SBA-15 upon SAC. The low angle XRD patterns of the corresponding samples also indicate absence of ordered mesopores (results not shown). All the silicalite-1 samples possess micropore area higher than 150 m^2/g due to the presence of zeolitic micropores (Table 1). Micropore area and micropore volume increase when the TPAOH/Si ratio is increased from 0.063 to 0.25. However, when the molar ratio is increased further to 0.5, both micropore area and micropore volume decrease. The silicalite-1 sample obtained with TPAOH/Si molar ratio of 0.25 exhibits a distinctively visible hysteresis loop. This hysteresis appears at relative pressure greater than 0.9 and indicates presence of pores larger than micropores. Further this particular silicalite-1 sample possesses relatively higher BET surface area, micropore area, total pore volume and micropore volume. Hence TPAOH/Si molar ratio, 0.25 was selected to prepare silicalite-1 from other silica sources also. In the present study, since no alkali hydroxide is used to prepare the dry gel, TPAOH acts not only as a structure directing agent but also as a mineralizer. In zeolite synthesis, the mineralizer plays an important role in forming silicate mobile species,

conveying chemical reactivity between silicate species and in stabilizing the final solid material[39]. Hence, when TPAOH concentration is altered, it will have some effect on reactivity of silicate species and growth of the zeolite crystal. This may be the reason for the changes seen in the porosity of the obtained zeolites on changing the concentration of TPAOH.

Nitrogen adsorption isotherms and pore size distribution curves of silicalite-1 samples prepared from different silica sources with TPAOH/Si molar ratio of 0.25 are compared in Fig.7(a). All the samples exhibit type I isotherm and possess H1 type hysteresis loop with the exception of the sample prepared from SBA-15. The position of the hysteresis loop shows the presence of pores in meso- and macro-pore regions. The BJH desorption pore size distribution curves of the samples are presented in Fig. 7(b). The data show that all the silicalite-1 samples possess wide pore size distribution, which falls in meso- and macro-pore region as classified by IUPAC. The upper limit of the pore size could not be deduced due to the limitations of the N_2 adsorption technique. The shape of the isotherm of silicalite-1 obtained from fumed silica (Fig.7(a)) is different from that of the others. In this sample, the adsorption increases more steeply in the mesopore region. Further, the shape of the t-plot (not shown) and data derived from it (Table 2) indicate absence of micropores, suggesting that the micropores of this sample may be covered with amorphous silica although the XRD patterns clearly show the presence of MFI topology (Fig. 3). Such kind of coating of amorphous layer covering the zeolites crystals has been observed by Valtchev *et al.*[40] during the synthesis of LTA nanozeolite. From the above results we conclude that the prepared silicalite-1 samples have multimodal pore system since micro-, meso- and macro-pores are present. However, at present it is not clear whether there is any interconnectivity between the micro-, meso- and macro-pores.

HRSEM images of the silicalite-1

High resolution scanning electron microscope (HRSEM) images of silicalite-1 samples obtained from SBA-15 with different TPAOH/Si molar ratios are

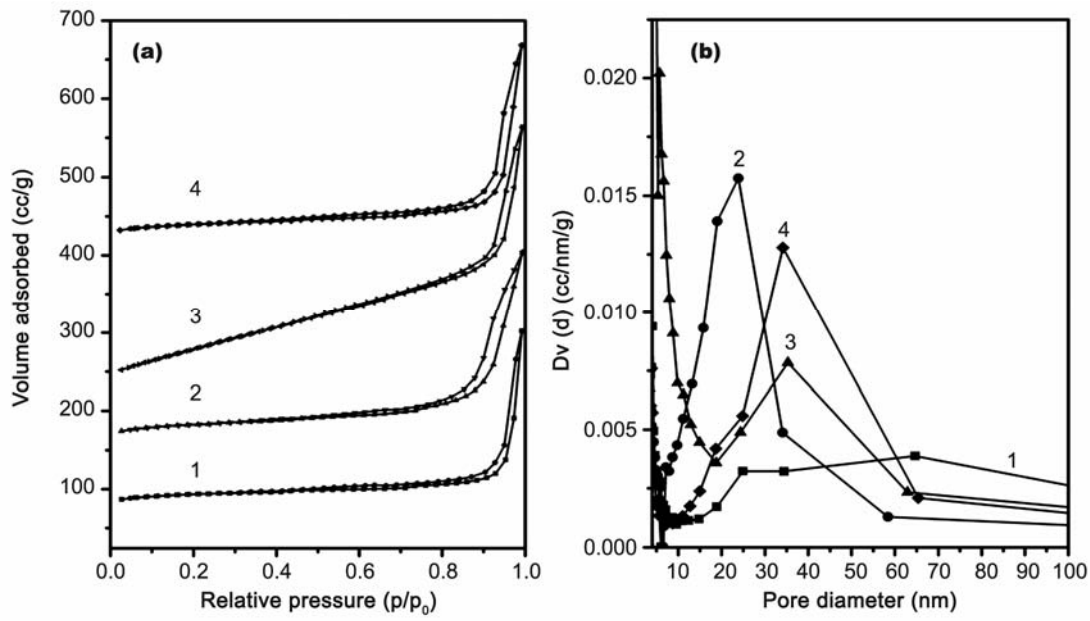

Fig. 7 – (a) N_2 adsorption isotherms and (b) BJH pore size distribution of silicalite-1 samples obtained from different silica sources. [TPAOH/Si molar ratio = 0.25. (1) SBA-15; (2) SBA-16; (3) fumed silica; (4) TEOS].

Table 2–N_2 adsorption data of silicalite-1 samples prepared from different silica sources with TPAOH/Si molar ratio of 0.25

No	Silica source	BET surface area (m^2/g)	Mesopore area (m^2/g)	Micropore area (m^2/g)	Micropore vol. (cc/g)	Total pore vol. (cc/g)
1	SBA – 15	274	47	226	0.123	0.46
2	SBA – 16	259	70	189	0.097	0.47
3	Fumed SiO_2	296	296	0	0	0.56
4	TEOS	271	64	207	0.110	0.49

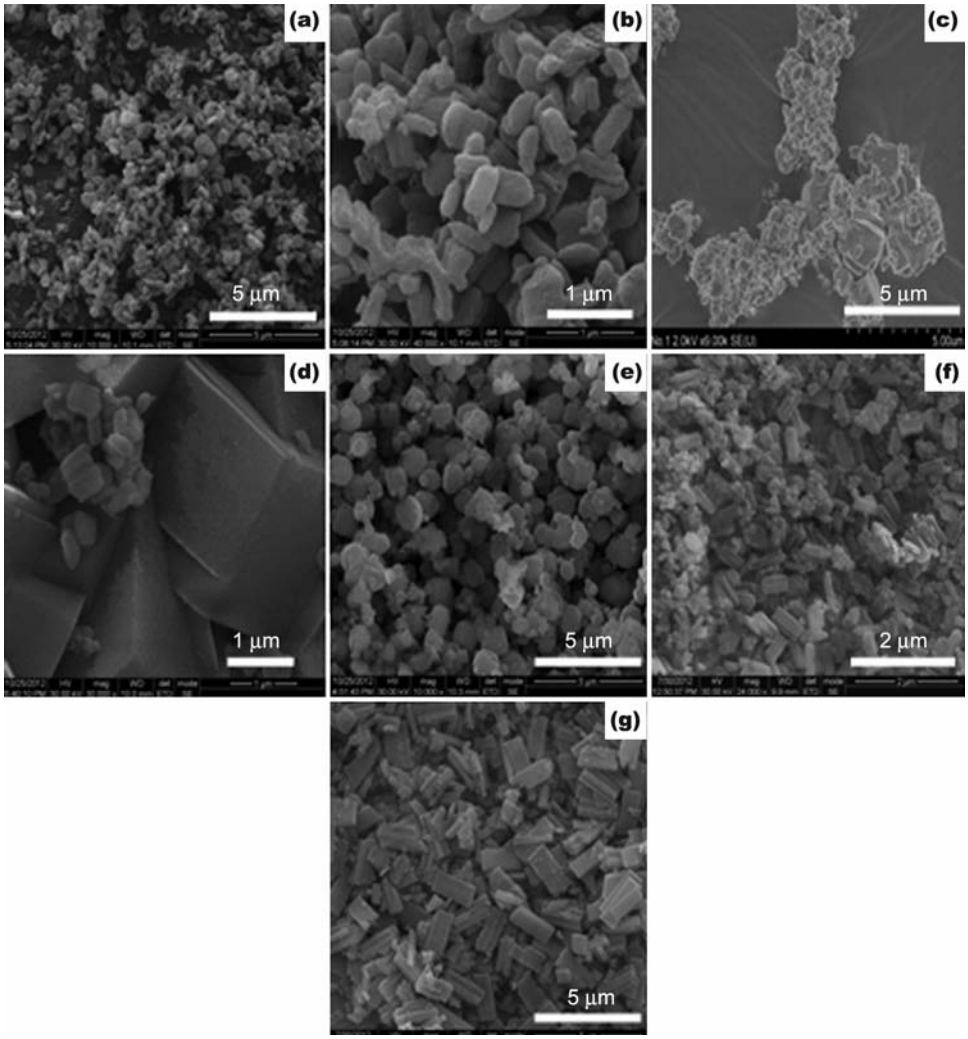

Fig. 8 – HRSEM images of crystallized dry gels obtained from SBA-15 with different TPAOH/Si molar ratios. [(a) & (b) 0.031; (c) & (d) 0.063; (e) 0.125; (f) 0.25; (g) 0.5].

presented in Fig. 8. When TPAOH/Si molar ratio is 0.031, the shape of the particles is similar to that of SBA-15 (Fig. 2 (a)). However, a closer look at the rod shaped particles reveals etching of the surface due to the action of the base, TPAOH. This observation along with XRD data (Fig. 3 (a)) suggests that the concentration of TPAOH is not sufficient for the crystallization of the silica into silicalite-1. While TPAOH/Si molar ratio is increased to 0.063, large micrometer sized silicalite-1 crystals along with particles similar to that observed under the TPAOH/Si molar ratio of 0.031 can be seen. This observation justifies the corresponding XRD pattern of this sample (Fig. 3 (b)), wherein diffraction by silicalite-1 crystals is obtained along with amorphous silica background. Increasing the molar ratio to 0.125 makes the rod shaped amorphous silica particles to disappear completely. Now the particles look crystalline and layer by layer growth can be visualized. At TPAOH/Si molar ratio of 0.25, typical coffin shaped zeolite crystals are observed along with rectangular shaped crystals. When the molar ratio is increased to 0.5, the crystals grow larger and become rectangular in shape. As discussed earlier under N_2 adsorption studies, TPAOH acts not only as a structure directing agent but also as a mineralizer. Hence, when the TPAOH concentration is altered, it will have some effect on the formation, shape and morphology of the zeolite crystals.

HRSEM images of silicalite-1 samples obtained from fumed silica, TEOS and SBA-16 under the same TPAOH/Si molar ratio of 0.25 are presented in Fig. 9. Silicalite-1 samples obtained from both fumed silica and TEOS are non-agglomerated nanocrystals. The morphology of silicalite-1 obtained from SBA-16 is different from others. In

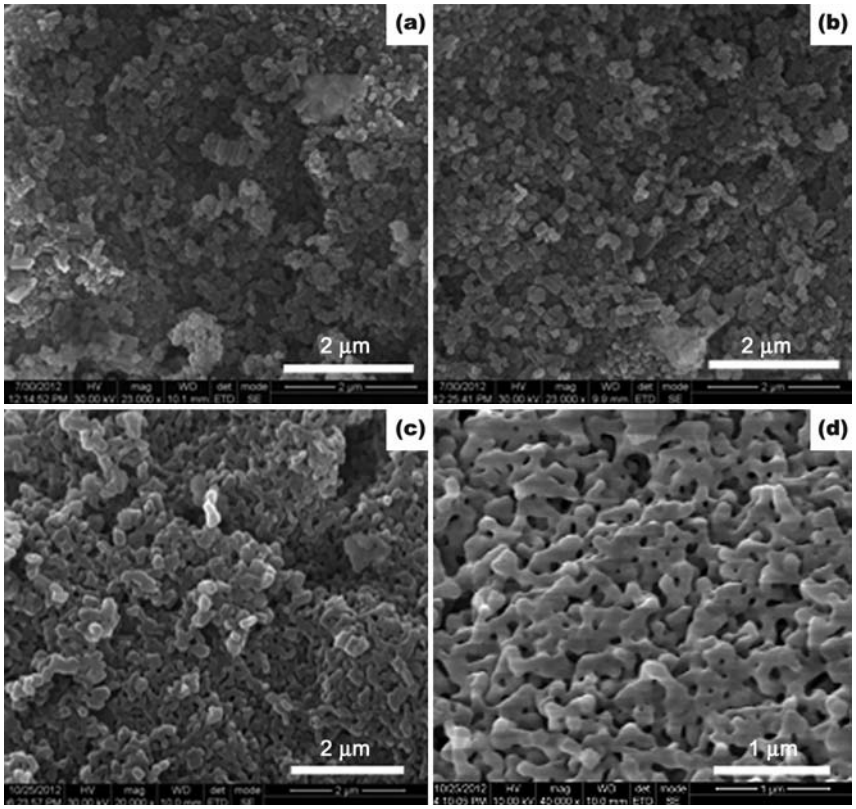

Fig. 9 – HRSEM images of silicalite-1 samples obtained from different silica sources. [TPAOH/Si molar ratio = 0.25. (a) fumed silica; (b) TEOS; (c) & (d) SBA-16].

this sample, the silicalite-1 crystals interconnect with each other and form a network like structure. This network arrangement creates macropores, which are clearly visible in the images. When comparing silicalite-1 samples prepared from the four different sources under the same TPAOH/Si molar ratio (0.25), it can be seen that SBA-15 yields relatively larger silicalite-1 crystals.

In summary, fumed silica and silica from TEOS, which mostly have interparticle porosity, yield non-agglomerated silicalite-1 nanoparticles with similar morphology and particle size. SBA-16, which has 3D cubic interconnected mesopore system and spherical morphology, yields interconnected silicalite-1 nanocrystals under the same SAC conditions. SBA-15, which has 2D hexagonal mesopore system, yields typical coffin shaped silicalite-1 crystals along with smaller rectangular nanoparticles under the same SAC conditions.

^{29}Si MAS NMR spectra of the dry gels

^{29}Si MAS NMR spectra of the dry gels, prepared under the TPAOH/Si molar ratio of 0.25 are presented in Fig. 10. The dry gels show a broad resonance from

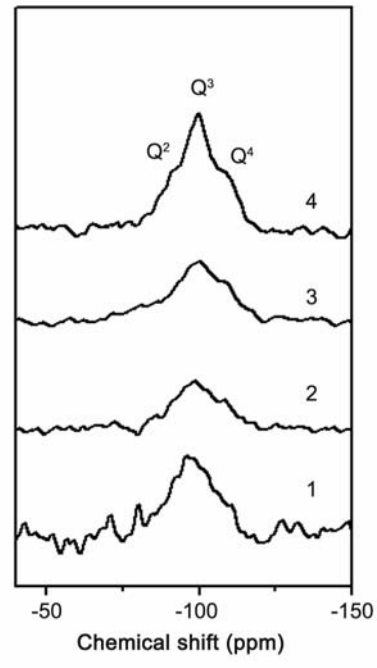

Fig. 10 – ^{29}Si MAS NMR spectra of the dry gels obtained from different silica sources. [TPAOH/Si molar ratio = 0.25. (1) TEOS; (2) fumed silica; (3) SBA-15; (4) SBA-16].

–70 to –120 ppm. This broad resonance indicates a mixture of different Si species[41]. The resonance peaks can be resolved into Q^2, Q^3, and Q^4 Si species appearing at –92, –99 and –108 ppm respectively[39]. Among the three Si species, Q^3 is dominant over Q^4. The lesser contribution from Q^4 species and the dominance of Q^3 species indicate partial hydrolysis of the original Q^4 species present in silicas into Q^3 species in the dry gel[41]. Comparison of the NMR spectra shows that the Si environments in the starting dry gels are almost similar.

As the dry gels already have some order as shown by ^{29}Si MAS NMR spectral data, preparation of silicalite-1 from dry gels by SAC can be viewed as transformation of a semi-ordered gel network into a well ordered zeolite network. The SAC method of preparation of zeolites can be considered as zeolite crystallization under hydrothermal conditions but in the absence of visible liquid phase[39]. Even though the mechanism of zeolite formation is similar for both conventional hydrothermal method and SAC method, there will be differences in these two methods for nucleation and crystal growth[39]. Compared to conventional hydrothermal method, in SAC method, lower mass transport limitations, high concentration gradients and high surface to volume ratio of the mobile phases are expected[39]. Such differences would cause changes in the formation rate, crystal morphology and state of aggregation[42,43]. The morphology and pore structure of the silica sources used in the present study are different. These differences may change mass transfer, concentration gradient and surface-to-volume ratio of the dry gels obtained from the sources. This may be the reason why the different silica sources yield silicalite-1 with different shapes and sizes under the same experimental conditions.

Conclusions

Morphology and pore structure of amorphous silica sources as well as concentration of tetrapropylammonium hydroxide used as both structure directing agent and mineralizer have a significant effect on the pore structure and morphology of silicalite-1 prepared by steam assisted conversion. The prepared silicalite-1 samples exhibit multimodal porosity as they have meso- and macro-pore apart from zeolitic micropores.

Acknowledgement

Thanks are due to Department of Science and Technology, Science and Engineering Research Board (DST-SERB), New Delhi, India for the financial support vide sanction letter No. SR/FT/CS-65/2011, dated 16.05.2012. One of the authors (MSMK) sincerely thanks VIT University, Vellore, India, for research associate fellowship. The authors also thank Sophisticated Analytical Instruments Facility (SAIF), Indian Institute of Technology Madras, Chennai, India, for HRSEM analysis and NMR Research Centre, Indian Institute of Science, Bangalore, India, for ^{29}Si MAS NMR analysis.

References

1 Davis M E, *Nature*, 417 (2002) 813.
2 Valtchev V, Smaihi M, Faust A C & Vidal L, *Angew Chem Int Ed*, 42 (2003) 2782.
3 Hartmann M, *Angew Chem Int Ed*, 43 (2004) 5880.
4 Parlett C M A, Wilson K & Lee A F, *Chem Soc Rev*, 42 (2013) 3876.
5 Holm M S, Esben Taarning, Egeblada K & Christensen C H, *Catal Today*, 168 (2011) 3.
6 Chen L H, Li X Y, Rooke J C, Zhang Y H,Yang X Y,Tang Y, Xiao F S & Su B L, *J Mater Chem*, 22 (2012) 17381.
7 Lopez-Orozco S, Inayat A, Schwab A, Selvam T & Schwieger W, *Adv Mater*, 23 (2011) 2602.
8 Hua Z L, Zhou J & Shi J L, *Chem Commun*, 47 (2011) 10536.
9 Serrano D P, Escola J M & Pizarro P, *Chem Soc Rev*, 42 (2013) 4004.
10 Xiao F S, Wang L, Yin C, Lin K, Di Y, Li J, Xu R, Su D S, Schlogl R, Yokoi T & Tatsumi T, *Angew Chem Int Ed*, 45 (2006) 3090.
11 Moller K, Yilmez B, Müller U & Bein T, *Chem Mater*, 23 (2011) 4301.
12 Na K, Jo C, Kim J, Cho K, Jung J, Seo Y, Messinger R J, Chmelka B F & Ryoo R, *Science* 333, (2011) 328.
13 Madsen C, Madsen C & Jacobsen C J H, *Chem Commun*, (1999) 673.
14 Schmidt I, Krogh A, Wienberg K, Carlsson A, Brorson M & Jacobsen C J H, *Chem Commun*, (2000) 2157.
15 Koo J B, Jiang N, Saravanamurugan S, Bejblová M, Musilová Z, Čejka J & Park S E, *J Catal*, 276 (2010) 327.
16 Holland B T, Abrams L & Stein A, *J Am Chem Soc*,121 (1999) 4308.
17 Wang Y, Tang Y, Dong A, Wang X, Ren N, Shan W & Gao Z, *Adv Mater*, 14 (2002) 994.
18 Lee Y J, Lee J S, Park Y S & Yoon K B, *Adv Mater*, 13 (2001) 1259.
19 Zhu H, Liu Z, Wang Y, Kong D & Yaun X & Xie Z, *Chem Mater*, 20 (2008) 1134.
20 Dong A, Wang Y, Tang Y, Ren N, Zhang Y, Yue Y & Gao Z, *Adv Mater*14, (2002) 926.
21 Zhang B, Davis S A, Mendelson N H & Mann S, *Chem Commun*, (2000) 781.
22 Ogura M , Shinomiya S Y, Tateno J, Nara Y, Kikuchi E & Matsukata M, *Chem Lett*, (2000) 882.
23 Abelló S, Bonilla A & Pérez-Ramírez J, *Appl Catal A*, 364 (2009) 191.
24 Zhou J, Hua Z, Cui X, Ye Z, Cui F & Shi J, *Chem Commun*, 46 (2010) 4994.

25 Li C, Wang Y, Shi B, Ren J, Liu X, Wang Y, Guo Y & Lu G, *Micropor Mesopor Mater*, 117 (2009) 104.

26 Xue C, Zhang F, Wu L & Zhao D, *Micropor Mesopor Mater*, 151 (2012) 495.

27 Wang Y, Tang Y, Dong A, Wang X, Ren N & Gao Z, *J Mater Chem*, 12 (2002) 1812.

28 Serrano D P, Aguado J, Escola J M, Rodriguez J M & Peral A, *Chem Mater*, 18 (2006) 2462.

29 Srivastava R, Iwasa N, Fujita S & Arai M , *Chem Eur J*, 14 (2008) 9507.

30 Xue Z, Zhang T, Ma J, Miao H, Fan W, Zhang Y & Li R, *Micropor Mesopor Mater*, 151 (2012) 271.

31 Matsukata M, Ogura M, Osaki T, Rao P R H P, Nomura M & Kikuchi E, *Top Catal*, 9 (1999) 77.

32 Alfaro S, Valenzuela M A & Bosch P, *J Porous Mater*,16 (2009) 337.

33 Moller K, Yilmaz B, Jacubinas R M, Muller U & Bein T, *J Am Chem Soc*, 133 (2011) 5284.

34 Meynen V, Cool P & Vansant E F, *Micropor Mesopor Mater*, 125 (2009) 170.

35 Treacy M M J and J.B.Higgins, *Collection of simulated XRD powder patterns for zeolites*, (Elsevier, Amsterdam) 2001.

36 Li C and Wu Z, *Hand book of zeolite science and technology* (Marcel Dekker Inc, New York) 2003, p. 435.

37 Lesthaeghe D, Vansteenkiste P, Verstraelen T, Ghysels A, Kirschhock C E A, Martens J A, Speybroeck V V & Waroquier M, *J Phys Chem C*, *112* (2008) 9186.

38 Xin H, Zhao J, Xu S, Li J, Zhang W, Guo X, Hensen E J M, Yang Q & Li C, *J Phys Chem C*, 114 (2010) 6553.

39 Cundy C S & Cox P A, *Micropor Mesopor Mater*, 82 (2005) 1.

40 Valtchev V P, Tosheva L & Bozhilov K N, *Langmuir*, 21 (2005) 10724.

41 Epping J D & Chmelka B F, *Curr Opin Colloid Interface Sci*, 11 (2006) 81.

42 Patel A K and Sand L B, *Molecular Sieves II*, (ACS, Washington) 1997, p.207.

43 Franklin K R & Lowe B M, *Zeolites*, 7 (1987) 135.